

3D model reconstruction and evaluation using a collection of points extracted from the series of photographs

Katarzyna Rzążewska

Faculty of Mathematics and Information Science
Warsaw University of Technology
Koszykowa 75, 00–662 Warszawa, Poland
Email: katarzyna@rzazewska.eu

Marcin Luckner

Faculty of Mathematics and Information Science
Warsaw University of Technology
Koszykowa 75, 00–662 Warszawa, Poland
Email: mluckner@mini.pw.edu.pl

Abstract—This work describes the whole process of 3D model reconstruction. It begins with the representation of the method that is used to find the matching between photographs and the methodology to use the data to form the initial structure of the reconstructed model, represented by a point cloud. As a next stage, a refinement process is performed, using the bundle adjustment method. A set of stereovision methods is used later on to find a more detailed solution. Those algorithms use pairs of images, therefore as a prerequisite a set of routines that aggregates those results is studied. The paper is concluded with a description of how the point cloud is processed, including the surface reconstruction, to form the result. The described methodology is illustrated with reconstructions of three series of professional photographs from a public repository and one series of amateur photographs created especially for this work. The results were evaluated by the proposed area matching and contour matching measures. **Index Terms**—3D Reconstruction, Image Matching, Epipolar Geometry, Features Extraction, Models Evaluation

I. INTRODUCTION

A RECONSTRUCTION of three dimensional (3D) models is one of the areas of the Computer Vision discipline that is quickly gaining momentum c.f. [1], [2], [3]. The development of information systems and the advancement in 3D graphics in general made it possible to create models that would depict real life objects. It has become even more important to be able to create models using two-dimensional photographs, taken using regular commodity digital cameras.

As one of the contributions of the following work, a computer tool has been developed that accomplishes the whole model reconstruction process. Out of a sequence of two-dimensional photographs, it can create a three dimensional full-colour model of the photographed object. The method is a mixture of algorithms based on features and solutions used in stereovision. The following project includes a description of this method. It also presents and comments on the results of applying the theory on a set of exemplary data series of digital photographs.

What follows is the main part of the work where the very process of 3D model reconstruction is explained. It begins with the representation of the method that is used to find the

matching between photographs and the methodology to use the data to form the initial structure of the reconstructed model, represented by a point cloud. As a next stage, a refinement process is performed, using the bundle adjustment method. A set of stereovision methods is used later on to find a more detailed solution. Those algorithms use pairs of images, so as a prerequisite a set of routines that aggregates those results is studied. The description is concluded with information about the cloud processing, including the surface reconstruction, to form the result.

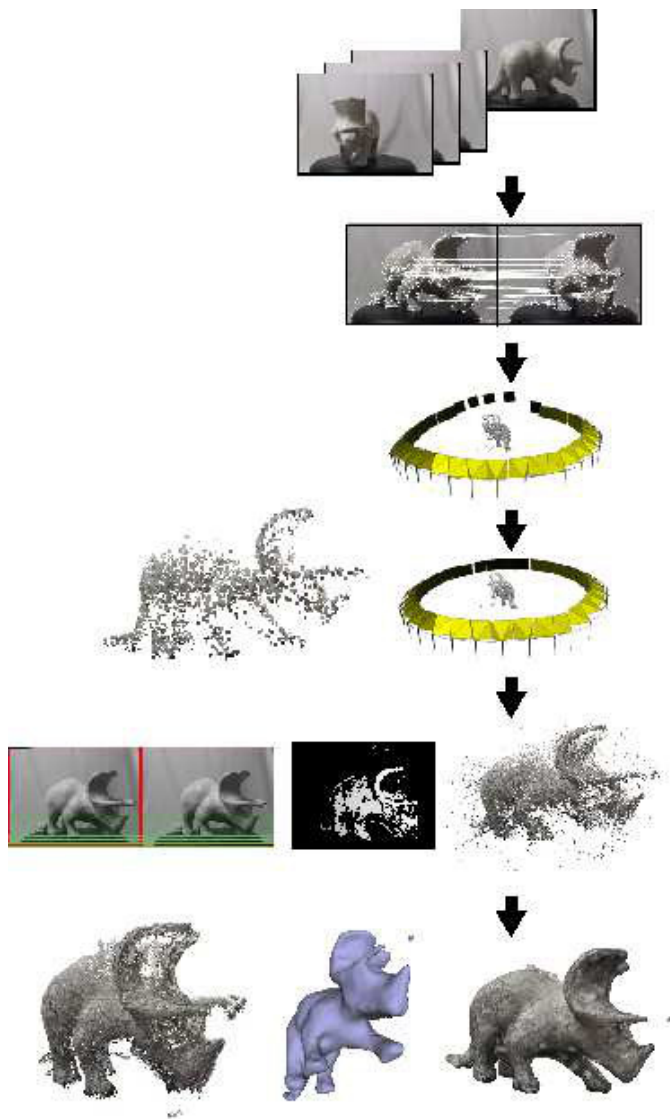
Each step of the process is illustrated with an exemplary image that show how the process progresses. This allows the reader to observe what the reconstruction process looks like. As an additional deliverable, a set of reconstructed models is presented. By comparing those images with the original models, the reader may decide on the quality of the process.

Several works present algorithms that result in high quality models. However, very often the reconstruction process bases on an expensive camera [2], specialist equipment such as a depth camera [3], or structured light [4].

The second important issue in the reconstruction based on computer vision algorithms (c.f. [5], [6], [7]) is lack of comparison methods. Very often, the result models are presented with evaluation of the quality different that visual comparison with the original object.

In this work, the proposed solution is based on low-cost algorithms and it is tested both on professional and amateur photographs. The snapshots from the four reconstructed model are presented in this work as well as the evaluation of their quality.

The paper is structured as follows. Section II presents basis of the epipolar geometry. The reconstruction process is briefly presented in Section III. The final models created from three series of photographs are described in Section IV and evaluated in Section V. Finally, the conclusions are presented in Section VI.



- 1) Input data (Section III-A)
- 2) Features detection and matching (Section III-B)
- 3) Structure and camera trajectory reconstruction (Section III-C)
- 4) Bundle adjustment (Section III-D)
- 5) Dense cloud creation (Section III-E)
- 6) Filtration and reconstruction (Section III-F)

Fig. 1. Reconstruction schema

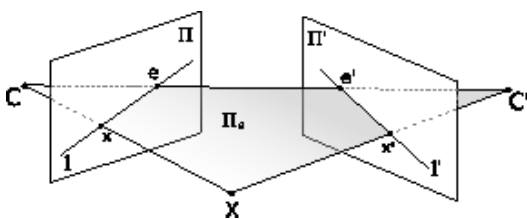


Fig. 2. Epipolar geometry defined by two cameras. C and C' – centres of cameras, Π and Π' – projection planes, e and e' – epipolar points, x and x' – projection of the point X on left and right view, l and l' – epipolar lines.

II. PRELIMINARIES

The reconstruction bases on the epipolar geometry and essential information about its theoretical aspects are given in this section. The basis of the epipolar geometry is given in Figure 2. A 3D point X has projections x and x' on two views. The point X , both views x and x' , and camera centres C and C' create the common plane. If the position of the point x is

known it is also known that the projection x' lies on the line l' . Therefore, the search for the point corresponding to x can be limited to the line l' .

The algebraic representation of epipolar geometry is given by the fundamental matrix F . The matrix describes mapping between a point and its epipolar line. The special form of the fundamental matrix is the essential matrix E . The matrix E is a fundamental matrix corresponding to the pair of normalised cameras. A normalised camera describes the relation between image points expressed in normalised coordinates and 3D points. The relation is represented as the camera matrix P .

An important component of the matrix P is the calibration matrix K . The internal parameters K of the camera may be extracted from the matrix P by the decomposition. The inversion of calibration matrix creates normalised point on the basis of a point from a picture. This transformation is used to create an initial cloud of points in the presented process.

Detailed information on the epipolar geometry and relations between the matrices are given in [8].



Fig. 3. Photographs from tested series

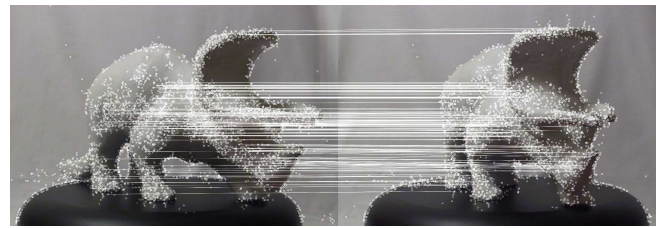
III. RECONSTRUCTION

The reconstruction process described in this work consists of several stages. The schema of the process is given in Figure 1. The process starts with input photographs. Next, the matching between the photographs is detected. Two next steps create sparse clouds. Before the final reconstruction, a dense cloud is created. In the final stage, after a filtration, a surface is reconstructed. More information about the stages is given in the following sections.

A. Input data

The reconstruction procedure was tested on three examples from the public repository [9] and one created especially for this work. The data sets are series of photographs. Each professional series consists of photographs of objects placed on an automated turntable and photographed every 5 degrees. The photographs have a high 3 M-pixels resolution acquired by two Canon Powershot G1 digital cameras.

In our experiments, two series 'Teddy bear' and 'Horse' were represented by the full set of 72 photographs. In the second series 'Dinosaur', the number of photographs was reduced to 35. The resolution of photographs is 842×822 and 1600×1200 for the first and the second series respectively.

Fig. 4. Matching for two photographs with 20° rotation

The last series 'Troll' is a bit different from the others. The object was immobile and the photographer was moving. The photographs were taken without a stand with an irregular angle. The resolution of photographs is 1200×800 . This series has only 33 photographs. The photographs were taken especially to test the reconstruction model presented in this work.

The three series present different approach to creation of data. The 'Teddy bear' and 'Horse' series are professional, detailed description of the objects. In the 'Dinosaur' series, photographs are still professional, but the number of images was reduced to decrease costs of documentation process. Both series were taken in a studio.

The 'Troll' series is an amateur documentation of the object created in an outdoor location.

Examples of photographs from all series are given in Figure 3.

B. Matching

In the first stage, relations between photographs are detected. The same points on multiple photographs are identified for that. In this work, the SURF method [10] was used to define characteristic points on the photographs. Other characteristic points that can be used in the matching are presented in [11].

The SURF detector localises characteristic points on the basis of the maximum value of Hessian. For selected points, horizontal and vertical Haar wavelets are calculated to fix an orientation. After these operations, a description of the point is created. The description is invariant from a scale and a rotation.

The matching consists in finding the common description of two points from different images. However, to avoid a false match the following steps are added.

All matches from the background are removed. Such matches are easy to detect, because positions of characteristics points are nearly constant in all photographs in a sequence.

The second group of removed matched is established on the basis of points without a dominant match. Such points have two or more equivalents on the second photography. If any of them is not distinctly better than the rest then all matches that start from this point are eliminated.

The next condition of the approval match is symmetry. The match between two points should be confirmed by two matching process. In the first process, the first photography is

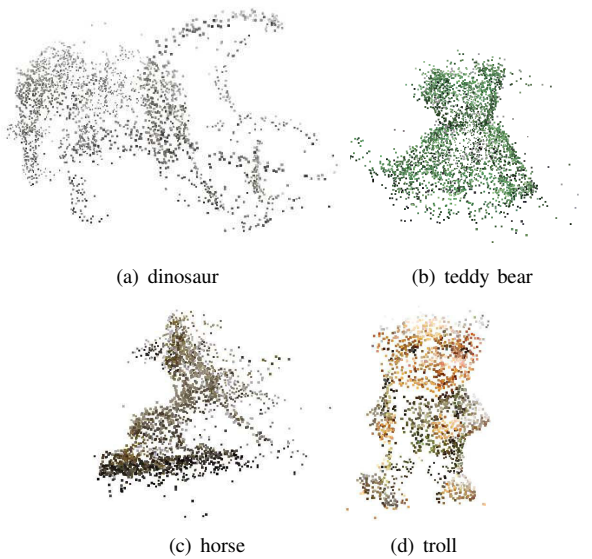


Fig. 5. Sparse clouds created in the reconstruction stage

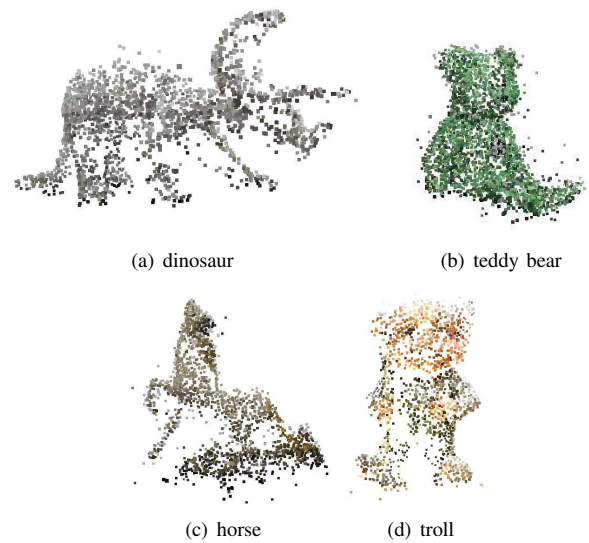


Fig. 6. Sparse clouds created in the bundle adjustment stage

taken as a source of characteristic points and the second one is area of searching for equivalents. In the second process, roles of photographs swap over.

All created matches should be confirmed by an epipolar model. The RANdom SAmple Consensus (RANSAC) approach [12] is used to detect the fundamental matrix. The matches that are inappropriate for the model are removed.

Finally, each match should be continued at least at three photographs. Each matched point from the second photograph should also be the beginning point for the subsequent math accepted in the matching process computing for the next pair of photographs.

The results of matching for a pair of photographs are presented in Figure 4. As can be seen, only a part of characteristic points have an approval match with a point from the second photograph.

C. Structure reconstruction

In the next stage, positions of detected points in 3D space are calculated as well as camera positions.

In practice, it is not enough to use the epipolar geometry to calculate positions of points separately for each pair of photographs. A calculation of the fundamental matrix is sensitive to noises and a detection of relations and translations between cameras results in errors cumulated in the final cloud.

To reduce the noises, the following solution is proposed.

A cloud of points is initiated by points localised on two first photographs. Each next photograph is used to add new points and calibrate the existing points from the cloud.

Before the calculation, coordinates of points from images are normalised. The normalised point is defined as $K^{-1}\mathbf{x}$, where \mathbf{x} is the coordinate in image space and K is a calibration matrix.

The K matrix is estimated as

$$K = \begin{bmatrix} w + h & 0 & \frac{w}{2} \\ 0 & w + h & \frac{h}{2} \\ 0 & 0 & 1 \end{bmatrix}$$

where w and h are width and height of image respectively. The same estimation was used in [13].

Next, for a selected pair of photographs the eight-point algorithm is used to calculate a fundamental matrix [8]. Owing the fact that coordinates were normalised the essential matrix can be used to detect relations between cameras.

Information about sequential photographs is added iteratively. However, now 2D points from a photograph are compared with 3D points from the created cloud. If a point has an equivalent in the cloud then the 3D coordinates are recalculated on the basis of a new observation. Otherwise, a new point can be added but only if it is present on at least three following photographs.

An important aspect of the reconstruction process is that it uses neither the camera position nor the fact of using a turntable pedestal.

The stage results in a cloud. Examples for analysed objects are given in Figure 5.

D. Bundle adjustment

The created clouds show recognisable views of the modelling objects. However, the density of clouds is not good enough to reconstruct object surface. Moreover, errors from this stage may propagate on the final model. Therefore, an additional stage is necessary to improve a quality of the cloud.

Such method is the bundle adjustment [14]. The method minimises the total mean squared error between real positions of points in a photograph and a position calculated from a 3D projection and a camera position. The algorithm operates on

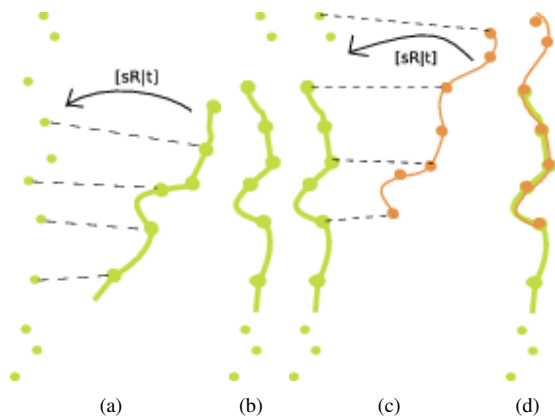


Fig. 7. Connection of the clouds:(a) the projection of the dense cloud on the sparse cloud, (b) the sparse cloud extended by the dense cloud, (c) the second dense cloud projected on the point of the sparse cloud matched to the first dense cloud, (d) the connected dense clouds.

the cloud calculated in the previous stage and camera parameters calculated using the Levenberg–Marquardt method [14].

The bundle adjustment is a general method. In this work, a specific implementation is used that calculates six parameters for each camera (three for a rotation and three for a translation) and three for each point from the cloud. Inner camera parameters are constant and common for all photographs.

This stage is optional, but definitely improves obtained results. In Figure 6, clouds after the bundle adjustment are presented. In the comparison with the previous clouds, objects are better visualised. However, clouds are still not dense enough to create a final reconstruction.

E. Dense cloud creation

The clouds created in the previous stages are too thin to reconstruct a high-quality surface. However, the clouds can be used to calculate a dense cloud, which will be a base for the final model.

The methodology used in this work bases on stereo block matching algorithms [15]. For a pair of photographs, equivalents of the same objects (pixels or small areas) should be localised on both photographs. A special transformation – rectification allows the algorithm to reduce a searching area to a line of even to a segment (under additional conditions) [16].

Collected data on the equivalents of points are stored as information about a distance between projections of points on a disparity map. With additional information about a camera localisation, the disparity map can be transformed into a depth map. The depth map codes information about the depth in the given point as an intensity.

In the 3D model reconstruction, many depth maps are connected and several problems arise in that process [17]. The maps are calculated for each pair of photographs. A relative small angle between the following photographs determines significant areas common for several maps.

The Iterative Closest Point technique [18] is commonly used to minimise the difference between two clouds of points. The

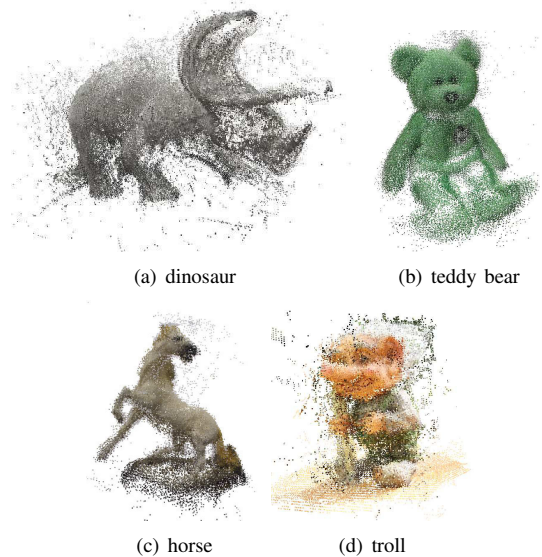


Fig. 8. Dense cloud created in the stage

algorithm uses the nearest neighbourhood criterion to find equivalents of an analysed point among clouds. Next, using a mean square cost function the transformation between clouds is solved. An iteration process is used to reduce the calculated cost.

When depth map are selected additional information is given and the connection process can be improved [19]. However, in this work, a new simple method that gives good results is proposed.

In the proposed method, clouds are connected together instead of disparity maps. Therefore, the filtration process plays major role in a quality of the final model. This solution is different that majority of solutions presented in other works, but a similar proposition can be found in [20].

Maps are transformed into dense clouds. Created cloud cannot be connected directly without creation of many noises. Therefore, the dense clouds are fitted in the sparse cloud created in the previous stage. Figure 7 presents the whole process.

The projection of the dense cloud to the sparse clouds is the minimalisation problem:

$$\sum_i ||b_i - sR a_i - t||^2, \quad (1)$$

where a_i is a point from the sparse cloud, b_i an equivalent of the point in the dense cloud. The solution is the transformation that consists of the rotation R , the translation t , the scale s , and minimalises the formula (1).

The results of the stage are given in Figure 8. The created clouds are dense, but noisy. The noises will be removed in the next stage.

F. Surface reconstruction

In the first step of the final stage, the dense cloud is filtered. Several algorithms are used to improve a quality of the cloud:

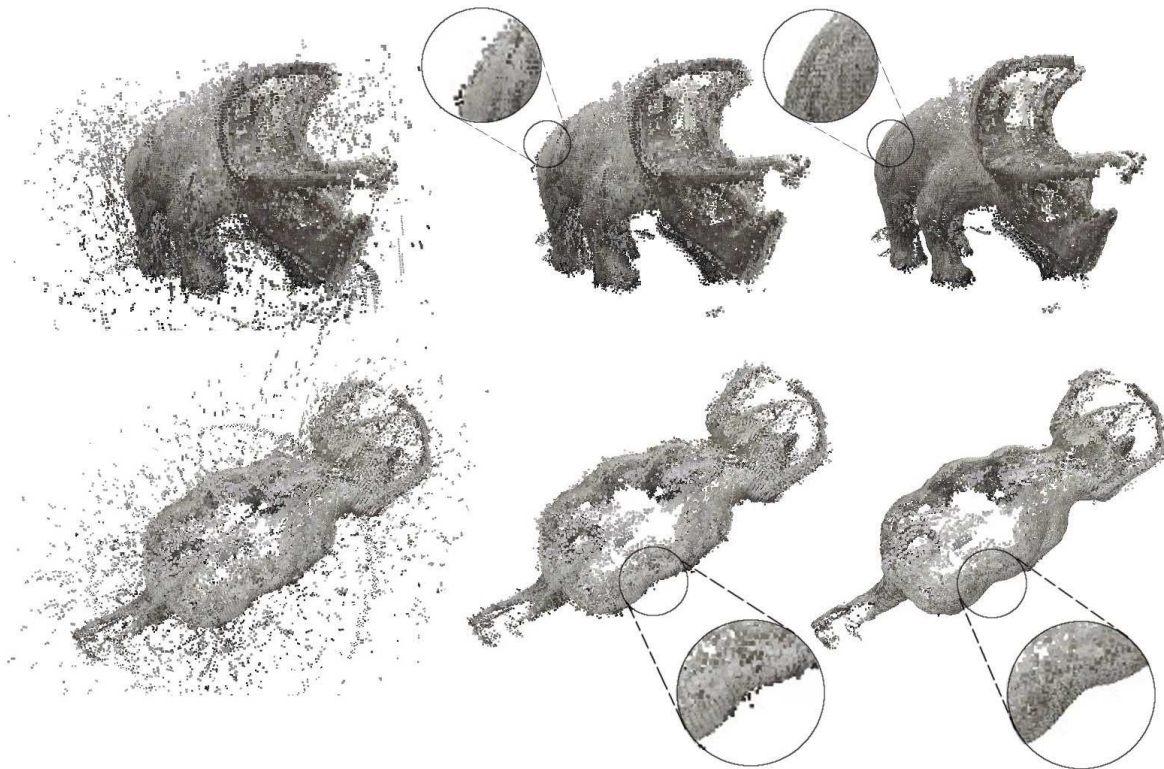


Fig. 9. Filtration. From the left: dense cloud, results of the SOR filter, and results of the MLS method.

the Statistical Outlier Removal filter, Voxel Grid filter, and the Moving Least Squares method.

The disparity maps have wide common areas. Therefore, points from an appropriate surface are located very dense. Otherwise, wrongly reconstructed points are located on random positions usually with small local density. Such points can be removed by the Statistical Outlier Removal filter [21]. For each point in the cloud, the filter calculates distances to k nearest neighbourhoods. On this base, a rejection threshold is calculated. When the average distance to the nearest points exceeds the threshold, a point is removed from the cloud.

The Voxel Grid filter reduces the number of points in the cloud. In a small neighbourhood, all points are reduced to a single point, which is the centroid.

Next, the cloud is smoothed. Noises near an appropriate surface could not be removed by the SOR filter. Therefore, the Moving Least Squares method [22] is used to remove the noises. In the method, a local surface is approximated and points are projected on the surface.

Effects of filtration are presented in Figure 9.

The last step is a surface reconstruction. The step is done by the Poisson method [23]. Before the reconstruction, normals for points should be calculated. The standard method that calculates normals [24] can be used. In the method, the Riemann graph is created with vertices defined by points and edges between nearest points. The graph forms the basis for a propagation of normals orientations.

The Poisson method creates a surface on the basis of the

cloud of points with oriented normals. The method solves for an approximate indicator function of the inferred solid, whose gradient best matches the normals. The output scalar function is then iso-contoured using adaptive marching cubes.

IV. RESULTS

The reconstruction time for a single model was about 6 minutes. The reconstructions were done on AMD Athlon 64 3000+ 2 GHz with Ubuntu system version 10.04.

The obtained results are presented in Figure 10. Reconstructed objects have good quality. Colours of triangles are interpolated from colours of corners. The colouring method is simple but brings satisfactory results. However, results show that a quality of the photography documentation influences the quality of the models.

The teddy bear (described by the full, professional documentation) is very well reconstructed including original depressions on its belly and back, while the horse model lost some details. In the dinosaur model (described by the professional, but reduced documentation), not all wrongly reconstructed points were removed. The model has a projection on its back. The troll model (described by the amateur documentation) has a distortion on the back. Moreover, a part of the stand was recognised as a part of the statue. Probably, this interpretation was caused by a shadow registered on the photographs. In a studio, this problem is eliminated.



Fig. 10. Reconstructed objects: Dinosaur, teddy bear, horse, and troll

V. EVALUATION

The main issue of the evaluation of created model is a lack of digital patterns to compare with the reconstruction. Therefore, we propose the following schema of models evaluation on the base of the series of photographs.

The projection of model was projected back on the cameras. As a result, the initial two dimensions projection was reconstructed. The reconstructed projection was compared with the isolated object from the origin photograph. Figure 11 presents all elements.

Both reconstructed object and isolated object from the origin photograph was used to create masks. The areas are compared and the model is evaluated using

$$q = \frac{b + c}{s}, \quad (2)$$

where b is the number of reconstructed pixels that are not a part of the origin object, c is the number of pixels from the origin object that are not reconstructed, and s is the number of matching pixels. Figure 12 presents all elements of the area matching.

The second proposed evaluation method is a contour matching. The contour matching analyses a reconstruction of details. For the created masks, the contour is calculated as the morphological gradient with the colour structuring element and with the 11 pixels diameter. Next, two evaluation measures were calculated:

$$q' = \frac{s}{m}, \quad (3)$$

where s is the number of matching pixels for both contours and m is the number of pixels in the model contour;

$$q'' = \frac{s}{o}, \quad (4)$$

where s is the number of matching pixels for both contours and o is the number of pixels in the object contour;

The measure q' (3) defines the percent of coverage of the object contour by the model contour, and the measure q'' (4) defines the percent of coverage of the model contour by the object contour.

Figure 13 presents all elements of the contour matching.

Table I presents evaluation of the models. We calculated averages of the evaluating coefficients for whole series of photographs. For the area matching coefficient q smaller values are better, for the contour matching coefficients higher values are better.

Studios objects have the similar area matching coefficients. The contour matching coefficients show that solid objects (the horse, the dinosaur) have better reconstructed contours than fluffy (teddy bear). The worst results were obtained for the troll model. It was caused by recognising the base of the model as a part of the model. When we edited model manually, we obtained better results.

TABLE I

EVALUATION OF THE MODELS: q - AREA MATCHING COEFFICIENT, q' , q'' , CONTOUR MATCHING COEFFICIENTS

model	avg q	avg q'	avg q''
dinosaur	0.10	0.68	0.65
horse	0.15	0.72	0.72
teddy bear	0.11	0.57	0.57
troll	0.91	0.33	0.31
edited troll	0.35	0.51	0.47

VI. CONCLUSIONS

In this work, the 3D models creating from photographs was presented. The method describes all stages of the reconstruction process from the features detection and the matching, through the creation of a sparse 3D cloud and a dense cloud, until the filtration and the surface reconstruction. All stages were illustrated with examples of their products.

The whole solution was implemented on the basis of open source libraries: OpenCV, Point Cloud Library and Sparse Bundle Adjustment. However, in several points original solutions were used. Especially original approach was used to connect the dense points clouds into one cloud using the sparse cloud.

Although some noises can be observed after a close inspection on the dinosaur model and the troll has some distortions, the obtained coloured reconstructions are good-looking and results are rewarding.

The presented process, together with the created application allows user to create complex 3D models without any expensive staff and advanced software.

REFERENCES

- [1] K. Kolev, T. Brox, and D. Cremers, "Fast joint estimation of silhouettes and dense 3d geometry from multiple images," *IEEE Transactions on Pattern Analysis and Machine Intelligence*, vol. 34, no. 3, pp. 493–505, 2012. [Online]. Available: <http://lmb.informatik.uni-freiburg.de/Publications/2012/Bro12>
- [2] D. Zawieska, "Analysis of operators for detection of corners set in automatic image matching," *Archives of Photogrammetry, Cartography and Remote Sensing*, vol. 22, pp. 423–436, 2011.
- [3] I. Y. Jang, J.-H. Cho, and K. H. Lee, "3d human modeling from a single depth image dealing with self-occlusion," *Multimedia Tools Appl.*, vol. 58, no. 1, pp. 267–288, 2012.
- [4] P. Lavoie, D. Ionescu, and E. Petriu, "3d object model recovery from 2d images using structured light," *Instrumentation and Measurement, IEEE Transactions on*, vol. 53, no. 2, pp. 437–443, April 2004.
- [5] S. Gimjumba, W. Narkbuekaew, M. Sangworasil, and C. Pintavirooj, "3d modeling from multiple projections with arbitrary-posed camera," in *Industrial Electronics and Applications, 2006 IST IEEE Conference on*, May 2006, pp. 1–5.
- [6] Y.-K. Zhang and Y. Xiao, "A practical method of 3d reconstruction based on uncalibrated image sequence," in *Signal Processing, 2008. ICSP 2008. 9th International Conference on*, Oct 2008, pp. 1368–1371.
- [7] H. M. Nguyen, B. Wunsche, P. Delmas, C. Lutteroth, and W. van der Mark, "High resolution 3d content creation using unconstrained and uncalibrated cameras," in *Human System Interaction (HSI), 2013 The 6th International Conference on*, June 2013, pp. 637–644.
- [8] R. I. Hartley and A. Zisserman, *Multiple View Geometry in Computer Vision*, 2nd ed. Cambridge University Press, 2004.
- [9] J. A. Pierre Moreels, "3D objects on turntable," www.vision.caltech.edu/pmoresels/Datasets/TurntableObjects/, 2006.
- [10] H. Bay, T. Tuytelaars, and L. V. Gool, "Surf: Speeded up robust features," in *In ECCV*, 2006, pp. 404–417.



Fig. 11. Evaluation preprocessing: the reconstructed projection, the original photograph, and the isolated object

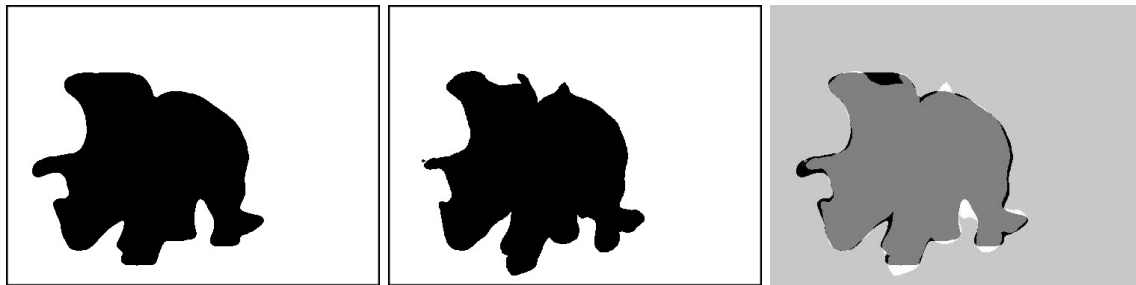


Fig. 12. Area matching: the mask from the origin photograph, the mask of the reconstructed object, and matched areas

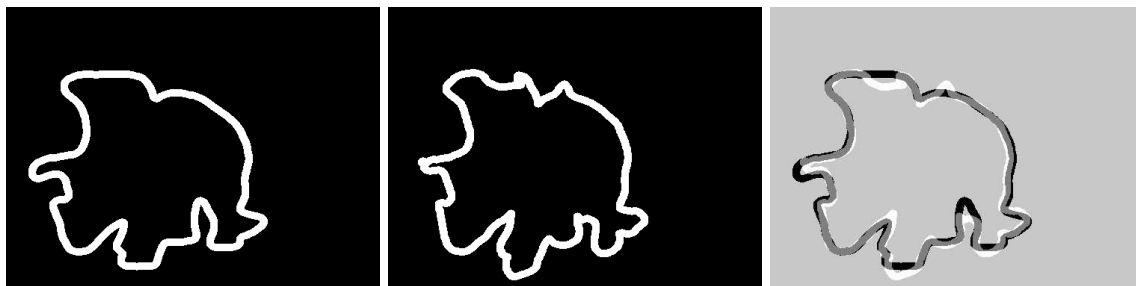


Fig. 13. Contour matching: the contour from the origin photograph, the contour of the reconstructed object, and the matched contours

- [11] G. Bagrowski and M. Luckner, "Comparison of corner detectors for revolving objects matching task," in *ICAISC (1)*, ser. Lecture Notes in Computer Science, L. Rutkowski, M. Korytkowski, R. Scherer, R. Tadeusiewicz, L. A. Zadeh, and J. M. Zurada, Eds., vol. 7267, Springer, 2012, pp. 459–467.
- [12] M. A. Fischler and R. C. Bolles, "Random sample consensus: a paradigm for model fitting with applications to image analysis and automated cartography," *Commun. ACM*, vol. 24, no. 6, pp. 381–395, Jun. 1981.
- [13] M. Pollefeys, "Visual 3d modeling from images," <http://www.cs.unc.edu/~marc/tutorial/>, course/Tutorial notes, presented at Siggraph 2002/2001/2000, 3DIM 2001/2003, ECCV 2000.
- [14] M. A. Lourakis and A. Argyros, "SBA: A Software Package for Generic Sparse Bundle Adjustment," *ACM Trans. Math. Software*, vol. 36, no. 1, pp. 1–30, 2009.
- [15] S. M. Seitz, B. Curless, J. Diebel, D. Scharstein, and R. Szeliski, "A comparison and evaluation of multi-view stereo reconstruction algorithms," <http://vision.middlebury.edu/mview/>, Washington, DC, USA, pp. 519–528, 2006.
- [16] B. Cyganek and P. Siebert, *An Introduction to 3D Computer Vision Techniques and Algorithms*. John Wiley & Sons, 2009.
- [17] D. Scharstein and R. Szeliski, "A taxonomy and evaluation of dense two-frame stereo correspondence algorithms," <http://vision.middlebury.edu/stereo/>, pp. 7–42, 2001.
- [18] S. Rusinkiewicz and M. Levoy, "Efficient variants of the ICP algorithm," in *Third International Conference on 3D Digital Imaging and Modeling (3DIM)*, Jun. 2001.
- [19] D. Bradley, T. Boubekeur, T. Berlin, and W. Heidrich, "Accurate multi-view reconstruction using robust binocular stereo and surface meshing," in *In Proc. of CVPR*, 2008.
- [20] K. S. Arun, T. S. Huang, and S. D. Blostein, "Least-squares fitting of two 3-d point sets," *IEEE Trans. Pattern Anal. Mach. Intell.*, vol. 9, no. 5, pp. 698–700, May 1987. [Online]. Available: <http://dx.doi.org/10.1109/TPAMI.1987.4767965>
- [21] R. B. Rusu, Z. C. Marton, N. Blodow, M. Dolha, and M. Beetz, "Towards 3d point cloud based object maps for household environments," *Robotics and Autonomous Systems Journal (Special Issue on Semantic Knowledge)*, vol. 56, pp. 927–941, 2008. [Online]. Available: <http://files.rbrusu.com/publications/Rusu08RAS-Semantic.pdf>
- [22] M. Alexa, J. Behr, D. Cohen-or, S. Fleishman, D. Levin, and C. T. Silva, "Computing and rendering point set surfaces," *IEEE Transactions on Visualization and Computer Graphics*, vol. 9, pp. 3–15, 2003.
- [23] M. Kazhdan, M. Bolitho, and H. Hoppe, "Poisson surface reconstruction," in *Proceedings of the fourth Eurographics symposium on Geometry processing*, ser. SGP '06, 2006, pp. 61–70.
- [24] H. Hoppe, T. DeRose, T. Duchamp, J. McDonald, and W. Stuetzle, "Surface reconstruction from unorganized points," in *SIGGRAPH Comput. Graph.*, 1992, pp. 71–78.